Journal of Cardiovascular Computed Tomography xxx (xxxx) xxx–xxx

Contents lists available at ScienceDirect

Journal of Cardiovascular Computed Tomography

journal homepage: www.elsevier.com/locate/jcct

Technical note

4D MDCT in the assessment of the tricuspid valve and its spatial relationship with the right coronary artery: A customized tool based on computed tomography for the planning of percutaneous procedures

Omar A. Pappalardo[a], Emiliano Votta[b], Matteo Selmi[b,c], Giovanni B. Luciani[c], Alberto Redaelli[b], Victoria Delgado[d], Jeroen J. Bax[d], Nina Ajmone Marsan[d,**]

[a] 3D and Computer Simulation Laboratory, IRCCS Policlinico San Donato, Italy
[b] Department of Electronics, Information and Bioengineering, Politecnico di Milano, Italy
[c] Scienze Chirurgiche Odontostomatologiche e Materno-Infantili, Università degli Studi di Verona, Italy
[d] Leiden University Medical Center, LUMC, Department of Cardiology, Leiden, the Netherlands

ARTICLE INFO

Keywords:
Tricuspid valve
Right coronary artery
Annulus
Tenting volume
MDCT

ABSTRACT

Multidetector computed tomography (MDCT) is currently the imaging technique of choice for the assessment of tricuspid valve (TV) annulus geometry and relationship with the right coronary artery (RCA). However, standardized protocols with a full 3D analysis are still lacking to plan percutaneous procedures for functional tricuspid regurgitation (FTR). A novel customized 4-dimensional tool based on MDCT data was developed and provided accurate information on TV annulus morphology (3D-perimeter, 2D-Area, maximum and minimum diameters, eccentricity index), function and distance to the RCA, crucial for patient selection of percutaneous TV procedures.

1. Introduction

New percutaneous procedures for the treatment of functional tricuspid regurgitation (FTR) mostly target the tricuspid valve (TV) annulus in order to re-shape or re-size it either through stitches or corkscrews. Since the right coronary artery (RCA) runs close to the TV annulus, these procedures are affected by a risk of RCA impingement.[1] Hence, screening of potential candidates for these procedures and pre-procedural planning should include the evaluation of TV annulus geometry and dynamics, as well as of TV annulus-RCA geometrical relationship. However, standardized protocols with a full 3D analysis are still lacking to plan percutaneous procedures for FTR and volumetric datasets are still used to obtain 2D cut-planes.[2,3] We therefore developed a novel MDCT-based software, designed to provide full 3D-analysis of the TV and overcome the above-mentioned limitations. We applied this software in patients with and without severe FTR to assess i) 3D TV annular geometry and dynamics during the cardiac cycle and ii) the spatial relationship between TV annulus and RCA.

2. Materials and methods

2.1. Patient population

Among patients who were clinically referred for an MDCT scan prior to transcatheter aortic valve replacement, 16 patients (5 males; age: 77 ± 9 years; body surface area: 1.8 ± 0.2 m^2) with severe FTR were randomly selected. Patients with pacemaker or implantable cardioverter-defibrillator leads were excluded. In addition, 11 patients without tricuspid regurgitation (7 males; age: 79 ± 8 years; body surface area: 1.8 ± 0.1 m^2) were included in the analysis as controls. MDCT examinations in all patients were performed on a 320-slice MDCT scanner using the protocol described in.[3]

2.2. MDCT data analysis

Each MDCT sequence was reorganized as a 4D-dataset consisting of volumetric data, with an average in-plane resolution of 0.38 mm and a mean slice thickness of 1.6 mm, over 10 frames of the RR interval. Morphological analysis was performed at mid- and late-systole and mid- and late-diastole.

Each 4D-dataset was initially navigated using the open-source

* Corresponding author.
E-mail address: n.ajmone@lumc.nl (N. Ajmone Marsan).

https://doi.org/10.1016/j.jcct.2020.04.003
Received 25 February 2020; Accepted 8 April 2020

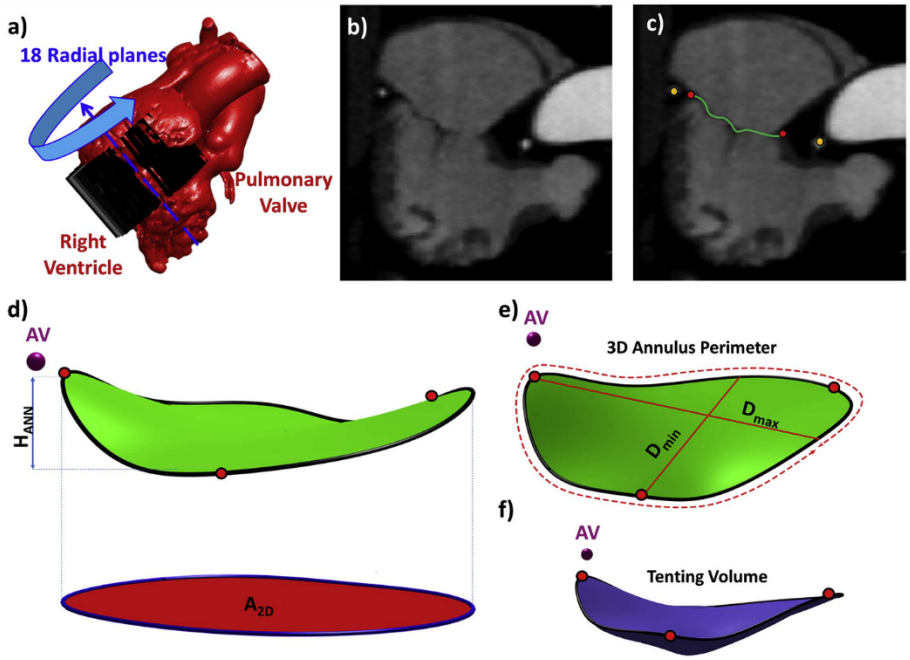

Fig. 1. MDCT data analysis. **a)** 18 radial planes rotated along the TV axis. **b)** One of the radial planes used for the segmentation. **c)** Annulus (red points), leaflets profile (green line), right coronary artery section (yellow points). **d)** Height of the annulus ($\mathbf{H_{Ann}}$) and 2D-area ($\mathbf{A_{2D}}$). **e)** principal diameters ($\mathbf{D_{max}}$ and $\mathbf{D_{min}}$) and 3D-perimeter. **f)** Tenting volume defined as the portion of space delimited by the blue surface. The commissures are highlighted with red points and the aortic valve with a purple point (AV). (For interpretation of the references to color in this figure legend, the reader is referred to the Web version of this article.)

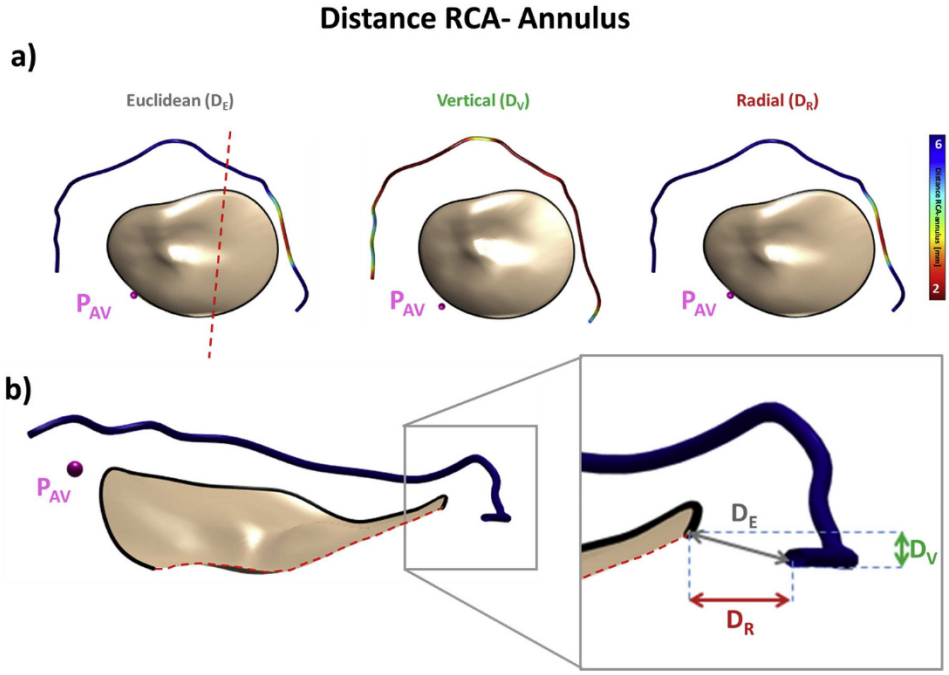

Fig. 2. a) Reconstruction of the RCA position in relation to the TV annulus. The color maps of the RCA represent the Euclidean($\mathbf{D_E}$), radial($\mathbf{D_R}$) and vertical($\mathbf{D_V}$) distance from the annulus while the dashed line highlights the cut section of the valve. **b)**Example of local $\mathbf{D_E}$, $\mathbf{D_V}$ and $\mathbf{D_R}$ between RCA and the TV annulus. (For interpretation of the references to color in this figure legend, the reader is referred to the Web version of this article.)

software 3D Slicer[4]: the long-axis 2- and 4-chamber planes were manually identified, and these planes were used to identify the true long-axis passing through the center of the TV. For the analysis of the morphology and the dynamics of the TV through the cardiac cycle, a custom software was developed using Matlab® (The Mathworks, Inc., Natick, MA, US). In specific, 18 planes evenly rotated around the TV axis, were automatically defined by interpolating the volumetric data (Fig. 1a). In all the analyzed frames and on each plane (Fig. 1b), 2 annular points were manually identified (Fig. 1c). At late systole, leaflets were manually traced and the section of the RCA was identified (Fig. 1c). In these reference frames, annular points were fitted through 4th order Fourier functions to obtain a continuous 3D annular profile.[5]

The following measurements of TV annulus dimensions were automatically computed at the defined four cardiac phases, (Fig. 1d-e):

- Maximum diameter ($\mathbf{D_{max}}$) and minimum diameter ($\mathbf{D_{min}}$)
- Height of the annulus ($\mathbf{Ha_{nn}}$), defined as the maximal extent of the annulus along the local z-axis
- Eccentricity index (**EI**), computed as ratio between $\mathbf{D_{min}}$ and $\mathbf{D_{max}}$
- 3D-perimeter
- 2D-area, defined as the area silhouetted by the projection of the annulus on the best-fit plane.

In addition, at late-systole 3D tenting volume was calculated as the portion of space limited by the 3D annulus plane and the leaflets surface (Fig. 1f) following the method described in.[6]

Finally, the 3D morphology of the RCA was defined interpolating the raw coronary points through a 3D natural cubic spline curve. For each point of the resulting curve, the 3D Euclidean distance to the TV

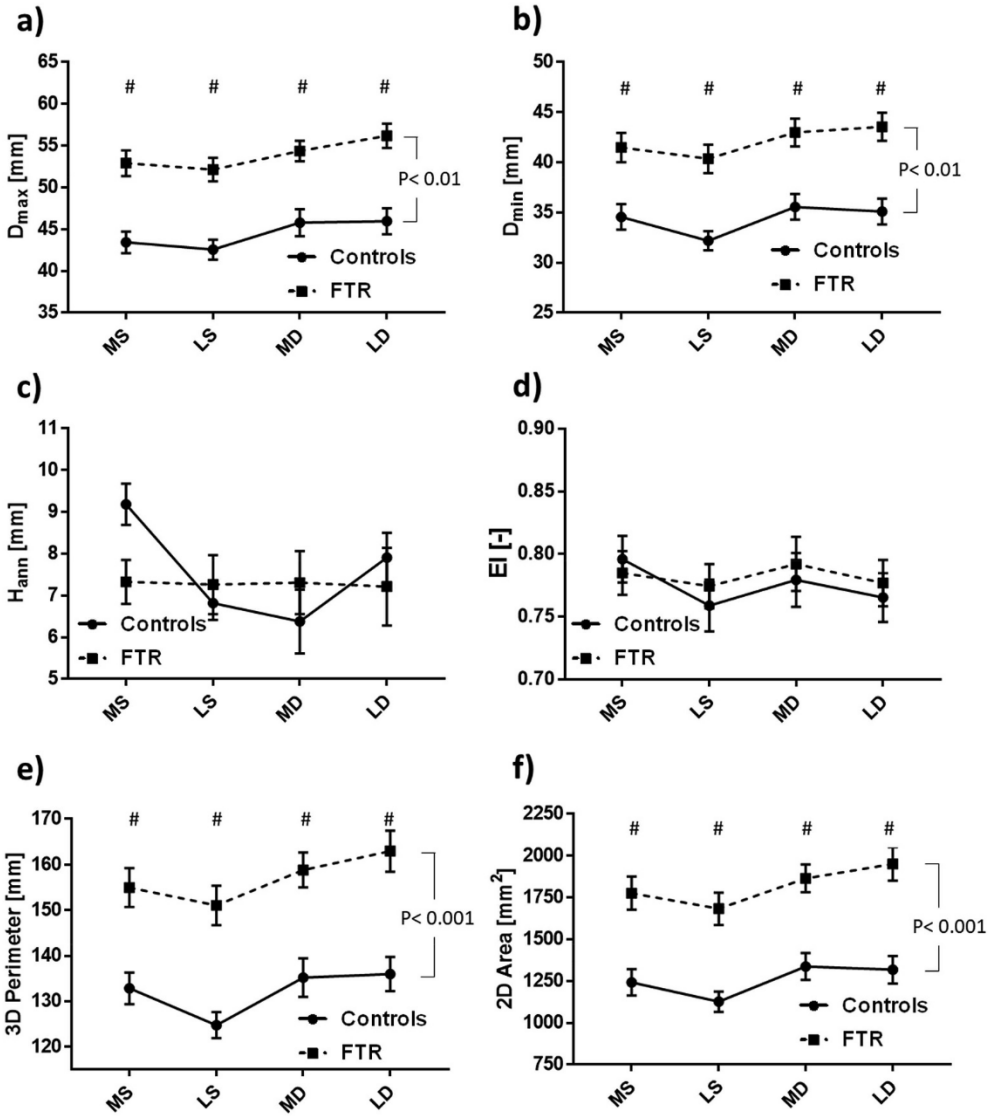

Fig. 3. TV morphological measurements in controls and FTR patients and their changes over the cardiac cycle: **a)** Maximum diameter ($\mathbf{D_{max}}$), **b)** Minimum diameter ($\mathbf{D_{min}}$), **c)** Height of the annulus ($\mathbf{H_{ann}}$), **d)** Eccentricity index (**EI**), **e)** 3D-perimeter, **f)** 2D-area. #, statistical difference between Controls and FTR at a given time point.

annulus was computed and decomposed into the corresponding vertical and radial components (Fig. 2).

2.3. Statistical data analysis

Statistical computations were performed using GraphPad Prism 7 (GraphPad Software Inc., La Jolla, CA, USA). Continuous variables were expressed as mean ± standard deviation (normal distribution). Dynamic changes of the TV parameters were assessed using 2-way ANOVA for repeated measures. Multiple comparison test were performed using Bonferroni test. Statistical significance was indicated by a $p < 0.05$.

3. Results

3.1. TV morphological and functional characterization

3D geometrical model of TV was successfully accomplished for all datasets (n = 27), supporting good feasibility of this approach even with different valve geometries. Dynamic changes in tricuspid annular dimensions over the cardiac cycle are shown in Fig. 3.

The comparison performed between FTR patients and controls confirmed that FTR is characterized by a significant dilatation of TV annulus, with larger 3D-perimeter, 2D-area, D_{max} and D_{min} (p-group, all < 0.05), consistent with previous studies,[7,8] also considering all time-points. For all these variables, phasic changes were also detected throughout the cardiac cycle (p-phase, all $p < 0.0001$) and in both groups statistically significant increase was observed from late-systole to mid-diastole (D_{max}: adjusted $p < 0.05$ in FTR patients and controls, respectively; D_{min}: adjusted $p < 0.001$; 3D-perimeter: adjusted $p < 0.0005$; 2D-area: adjusted $p < 0.0005$). Of interest, FTR and control patients shared almost equal EI values 0.8 ± 0.1 (p-group = 0.7550), which remained almost constant over the 4 considered time-points of the cardiac cycle (p-phase = 0.2501). In turn, differences in H_{ann} (p-group = 0.6901) between FTR patients and controls did not reach statistical significance. However, both groups showed markedly different trends in time: in controls, H_{ann} significantly decreased from mid-systole (9.2 ± 1.6 mm) to late-systole (6.8 ± 1.3 mm), remained almost unchanged in mid-diastole (6.4 ± 2.5 mm), and re-increased in late-diastole (7.9 ± 2.0 mm). Overall these results suggest that in FTR patients annular dilation occurs maintaining the original valve shape also during the cardiac cycle,

but TV annulus tends to be flat during the whole cardiac cycle, without significant changes in height.

As expected, TV tenting volume was significantly larger in FTR patients (3.36 ± 2.74 ml) as compared to controls (0.85 ± 0.61 ml) and in agreement with the values reported by Sukmawan et al. [9] using echocardiography.

3.2. TV annulus-RCA geometrical relationship

The minimum distance between TV annulus and RCA was computed for all FTR patients with 3 methods and median values were 3.1 mm for Euclidean distance, 2.7 mm for its radial component and 0.8 mm for its vertical component. A statistically significant difference between the distances computed by the three methods was observed ($p < 0.0001$) being the vertical always the smallest.

The representative case shows the course of the RCA and the distance from the TV annulus computed with the Euclidean, vertical and radial method (Fig. 2, distance <2 mm is represented in red).

The distance between the TV annulus and RCA in FTR patients has been measured also by Rosendael et al.,[3] however, only at the level of the anterior and posterior TV leaflets insertion using a 2D cut-plane, thus overlooking the three-dimensionality of both structures. The variability we observed in the distance between RCA and TV annulus confirms that the entire course of RCA must be taken into consideration when analyzing its relationship with TV annulus. Moreover, Rosendael et al. computed this distance using either vertical or radial (horizontal) directions with respect to the annulus plane. In contrast, by exploiting the automatic computation of the Euclidean distance between the TV annulus and RCA, the approach was standardized for all the analyzed datasets, yielding the actual distance between the two structures along the entire course of the RCA. Such an accurate measure of the distance between the TV annulus and RCA may be of crucial importance in planning transcatheter procedures that target the TV annulus and potentially can damage the RCA.

4. Conclusions

The novel MDCT-based tool developed in the current study is able to perform a comprehensive and fully 3D analysis of the TV, providing precise information on morphology, function and spatial relationship with the RCA. This assessment is crucial for patient selection and planning of percutaneous TV procedures.

References

1. Díez-Villanueva P, Gutiérrez-Ibañes E, Cuerpo-Caballero GP, et al. Direct injury to right coronary artery in patients undergoing tricuspid annuloplasty. *Ann Thorac Surg.* 2014;97(4):1300–1305. https://doi.org/10.1016/j.athoracsur.2013.12.021.
2. van Rosendael PJ, Delgado V, Bax JJ. The tricuspid valve and the right heart: anatomical, pathological and imaging specifications. *EuroIntervention.* 2015;11:W123–W127. https://doi.org/10.4244/EIJV11SWA35.
3. van Rosendael PJ, Kamperidis V, Kong WKF, et al. Computed tomography for planning transcatheter tricuspid valve therapy. *Eur Heart J.* 2016;38(9):ehw499https://doi.org/10.1093/eurheartj/ehw499.
4. Pieper S, Lorensen B, Schroeder W, Kikinis R. *The NA-MIC Kit: ITK, VTK, Pipelines, Grids and 3D Slicer as an Open Platform for the Medical Image Computing Community.* 2006; 2006:698–701 2006.
5. Sturla F, Onorati F, Puppini G, et al. Dynamic and quantitative evaluation of degenerative mitral valve disease: a dedicated framework based on cardiac magnetic resonance imaging. *J Thorac Dis.* 2017;9. https://doi.org/10.21037/jtd.2017.03.84.
6. Jaworek M, Pappalardo OA, Selmi M, et al. Treatment of tricuspid regurgitation at subvalvular level: hemodynamic and morphological assessment in ex-vivo beating heart model. *Structural Heart.* 2020;4(1):36–45. https://doi.org/10.1080/24748706.2019.1686555.
7. Hinzpeter R, Eberhard M, Burghard P, et al. Computed tomography in patients with tricuspid regurgitation prior to transcatheter valve repair: dynamic analysis of the annulus with an individually tailored contrast media protocol. *EuroIntervention.* 2017;12(15):e1828–e1836. https://doi.org/10.4244/EIJ-D-16-00891.
8. Ton-Nu T-T, Levine RA, Handschumacher MD, et al. Geometric determinants of functional tricuspid regurgitation: insights from 3-dimensional echocardiography. *Circulation.* 2006;114(2):143–149. https://doi.org/10.1161/CIRCULATIONAHA.106.611889.
9. Sukmawan R, Watanabe N, Ogasawara Y, et al. Geometric changes of tricuspid valve tenting in tricuspid regurgitation secondary to pulmonary hypertension quantified by novel system with transthoracic real-time 3-dimensional echocardiography. *J Am Soc Echocardiogr.* 2007;20(5):470–476. https://doi.org/10.1016/j.echo.2006.10.001.